Anisotropic interactions and strain-induced topological phase transition in Sb_2Se_3 and Bi_2Se_3

Wenliang Liu, Xiangyang Peng,* Chao Tang, Lizhong Sun, Kaiwang Zhang, and Jianxin Zhong†
Laboratory of Quantum Engineering and Micro-Nano Energy Technology, Xiangtan University, Xiangtan 411105, Hunan Province, China
(Received 5 November 2011; published 9 December 2011)

Based on first-principles calculations, we study the dependence of topological phase on anisotropic interactions in Bi_2Se_3-type materials. By applying different strains in order to vary interactions, we reveal that the topological phase is insensitive to lateral interaction but can be effectively tuned by longitudinal interaction. Longitudinal strain is inhomogeneous in the studied systems. The interquintuple interaction plays a dominant role in determining the topological phase. We explain the puzzling band-topology difference between Sb_2Se_3 and Bi_2Se_3 and propose an approach to tuning the topological phase by strain. It is found that Sb_2Se_3 can be converted into a topological insulator by applying compressive longitudinal strain while the converse strain can turn Bi_2Se_3 into a normal insulator. We have studied thin films of Sb_2Se_3 and Bi_2Se_3 and also observed a strain-induced topological phase transition.

DOI: 10.1103/PhysRevB.84.245105 PACS number(s): 71.20.−b, 73.20.At, 73.43.Nq, 75.70.Tj

I. INTRODUCTION

Bi_2Se_3, Bi_2Te_3, and Sb_2Te_3 are-second generation topological insulators (TIs), featuring single Dirac cone at the Γ point.[1–4] Due to strong spin-orbit coupling (SOC), they possess protected surface states of Dirac fermions and simultaneously retain a bulk energy gap.[5–8] These unconventional properties open a new avenue to applications in spintronics and quantum computing.[6,7,9,10] Bi_2Se_3-type materials share a rhombohedral layered structure, in which five covalently bonded atomic layers are grouped into a quintuple layer (QL) and the QLs are weakly bonded along the c axis to form a crystal.[11,12] This structure is marked by highly anisotropic bonding in lateral and longitudinal directions and within and between the QLs. Although Bi_2Se_3-type TIs have been the focus of many current studies,[13–17] there is an important question still to be addressed, i.e., how the topological phase is dependent on anisotropic interactions in these materials.

One can vary the anisotropic interactions by applying strains in different directions[18,19] and investigate the above-mentioned question through the study of strained systems. A clue to the answer may be found in the band topology difference between Bi_2Se_3 and Sb_2Se_3. They both are of the same structure and contain heavy atoms that could lead to strong SOC. Sb_2Se_3 is expected to be a TI in many ways. However, it is identified to be a normal insulator (NI),[11] posing an interesting and puzzling exception. This implies that, apart from the heavy elements in these materials, there is another underlying mechanism governing the topological phase. Looking into the lattice parameters, one can find that Sb_2Se_3 and Bi_2Se_3 have c/a ratios of 7.318 and 6.921,[11] respectively. The QLs are more closely packed in Bi_2Se_3, which possibly gives rise to stronger SOC and makes Bi_2Se_3 a TI. Therefore, a conjecture can be made that Sb_2Se_3 may be converted into a TI by applying compressive strain longitudinally along the c axis. This suggests that the interactions in the crystal, such as crystal-field and SOC, can be effectively tuned by strain, leading to topological phase transitions. Although there have been signatures that can, to some extent, indicate a topological phase transition of the strained bulk system,[17] we based our studies on a rigorous methodology by calculating the Z_2 topological invariant, which can unambiguously and directly identify topological phase. Furthermore, the protected Dirac cone of the topological surface states is the hallmark of TIs, which will lead to unique and important applications. Because strain widely exists in the surfaces and the interfaces, it would be interesting to know how the topological surface states vary with strain.

In this work, we have carried out first-principles calculations on strained Sb_2Se_3 and Bi_2Se_3. It is found that longitudinal interaction, especially the inter-QL interaction, dominates the topological phase, whereas lateral interaction and the interaction within a QL have little effect. We have studied both strained bulk systems and films and found a method to control the topological phase of Bi_2Se_3-type materials by strain. We explain the puzzling topological phase difference between Sb_2Se_3 and Bi_2Se_3. It is found that Sb_2Se_3 can be changed into a TI when compressively strained along the c axis while longitudinal expansion of the lattice can transform Bi_2Se_3 into an NI. It is also observed that strain can tune the topological surface states. The role of the interaction of the opposite surfaces of films is clarified.

II. COMPUTATIONAL DETAILS

The calculations are performed by using VASP[20,21] within the Perdew-Burke-Ernzerhof generalized gradient approximation (GGA-PBE).[22] The electron-core interaction is described by projector augmented wave (PAW) potentials.[23] The cutoff for plane-wave expansion is set to be 340 eV. SOC is taken into consideration. We studied both the bulk and thin films of Sb_2Se_3 and Bi_2Se_3. Whenever strain is applied, a hexagonal unit cell is used, which contains 3 QLs and 15 atoms for bulk and 8 QLs and 40 atoms for thin films. In the calculation for thin films, adjacent slabs are separated by a vacuum layer of 15 Å. The Brillouin zone is sampled by a Γ-centered mesh of $11\times11\times1$. Since Sb_2Se_3 and Bi_2Se_3 have an inversion center, their Z_2 topological invariant can be determined by parity analysis.[24] Under various strains, our calculations show that the parities of all occupied bands remain unchanged at time-reversal-invariant momenta other than the Γ point. Therefore, the system is a TI if the product of the parities of all occupied bands at the Γ point is negative. Otherwise, it is

an NI. In the following, we only discuss the parities at the Γ point.

III. RESULTS AND DISCUSSIONS

A. The topological phase transition in bulk systems

We first discuss the relationship between topological phase and anisotropic interactions in Sb_2Se_3. As a starting point, the unstrained system is studied to provide a reference for comparison. Since there are no experimental data available, we optimized the lattice parameters with GGA for Sb_2Se_3 by self-consistent calculation, which gives $a = 4.078$ Å and $c = 29.92$ Å. For comparison, we give here the corresponding lattice parameters by LDA (local density approximation), which are $a = 3.998$ Å and $c = 27.566$ Å. After van der Waals correction, the GGA lattice parameters become $a = 4.026$ Å and $c = 28.732$ Å. The c/a ratio obtained by GGA is closer to that obtained by GGA with van der Waals correction. Sb_2Se_3 is identified as an NI by using GGA in previous calculations.[11,25] To have a direct comparison, we choose to use GGA in our calculations. Moreover, it is found that the calculations of Bi_2Se_3 by GGA have better agreement with the experiments than those based on LDA,[26] suggesting that GGA might be more suitable for this type of material. Our parity analysis of the bulk primitive unit cell yields the same results as obtained in previous studies[11] [see Fig. 2(d) of Ref. 11]. The 3-QL hexagonal bulk unit cell has forty-two occupied bands (15 *s* bands and 27 *p* bands). Their parities are listed in Table I. The product of the parities of the occupied bands is positive, verifying that unstrained Sb_2Se_3 is an NI. The band structure is shown in Fig. 1(a) with a gap of 0.064 eV. In Fig. 1(e), the band structure of the unstrained 8-QL Sb_2Se_3 film is displayed. There is a small band gap of 0.026 eV at the Γ point, in good agreement with the previous calculations.[11]

To study the longitudinal interaction, a uniaxial strain along the c axis from -1% to -10% is applied to Sb_2Se_3 (bulk 3-QL unit cell). The minus sign here denotes compressive strain. As shown in Table I, the energy gap is reduced to 0.0034 eV when Sb_2Se_3 is strained by -1% along its c axis, indicating that this strained system is already very close to the topological phase transition point. However, it is still an NI because the product of the parities remains positive (see Table I). Figure 1(b) depicts the charge distribution of the highest occupied molecular orbital (HOMO) and the lowest unoccupied molecular orbital (LUMO) at the Γ point. The charge of the HOMO has a large distribution at the more electronegative anion atom Se, while the charge of the LUMO is mainly concentrated on the less electronegative cation atom Bi, which is typical of an NI. If the c-axis strain is increased to -2%, the gap does not continue to decrease. Instead, it is reopened to a value of 0.065 eV, suggesting that an inversion of the conduction and valence bands occurs and that Sb_2Se_3 has been converted into a TI. This is confirmed by our parity analysis. The product of the parities becomes negative and the parities of the LUMO and HOMO are inverted, as shown in Table I. One can clearly observe in Fig. 1(d) that the charge distributions of LUMO and HOMO are mainly located at Se and Bi atoms, respectively, which are directly opposite the distributions shown in Fig. 1(b). By this means, the band inversion can be directly illustrated. Under larger compressive strain along the c axis, the gap grows larger and larger and the system remains a TI [see Fig. 1(f) and Table I].

We have investigated how the phase transition is induced by strain. The topological phase mainly depends on the gap size λ_v (without SOC) and the strength of the SOC λ_{SO}.[5,17] For a TI, λ_v is small and λ_{SO} is large so that the band inversion can occur.[5,17] The size of the inverted band gap is proportional to λ_{SO}. Our calculations find that λ_v decreases from 0.15 eV to about 0.03 eV at -2% c-axis strain due to the change of the crystal field, and does not decrease much further under larger strain. The inverted band gap, on the other hand, continues to grow with the increase of longitudinal compression, indicating an increase of SOC strength. Therefore, not only by the change of the crystal field to reduce λ_v, but also by the increase of SOC strength λ_{SO}, compressive c-axis strain makes Sb_2Se_3 a TI.

We further apply lateral strains to the above systems to address the effect of lateral interaction. We exhibit here two systems under different lateral strains while their c-axis strains are fixed at -1% and -2%. Since the calculated Poisson's ratio is 0.25, -1% and -2% c-axis strains correspond to 0.25% and 0.5% lateral expansion, respectively. In our studies, the lateral strain is varied in a much wider range, from -2% to 2% ($\gg 0.25\%$ and 0.5%). Parity analysis shows that there is no change of the Z_2 topological invariant with respect to the lateral strains. In above discussions, Sb_2Se_3 is found to be an NI and a TI under uniaxial c-axis strains of -1% and -2%, respectively, and it remains so after lateral strains are applied. This indicates that the topological phase is quite insensitive to the lateral

TABLE I. The parity eigenvalues of the occupied bands (before the semicolon) and the lowest unoccupied band (after the semicolon) at the Γ point for Sb_2Se_3 and Bi_2Se_3 under longitudinal c-axis strains (listed in the fifth column). Positive and negative signs denote even and odd parity, respectively. The sign in parentheses is the product of the parity eigenvalues of the occupied bands. The calculated band gap is also shown in the third column. The nearly degenerate states at the Γ point are connected by the symbol $\widehat{\ }$.

Sb_2Se_3	0.0%	0.0643 eV	(+)	++−− +−++ −−+− ++−− +−+− ++−− −+−+ ++−− +−−+ −−++ −−;+
	−1.0%	0.0043 eV	(+)	++−− +−++ −−+− ++−− +−+− ++−− −+−+ ++−− +−−+ −−++ −−;+
	−2.0%	0.0649 eV	(−)	++−− +−++ −−+− ++−− +−+− ++−− −+−+ ++−− +−−+ −−++ −+;−
	−5.0%	0.1800 eV	(−)	+++− −−++ +−+− ++−− +−+− +−−− −+−− +−++ −++− +−++ ++;−
Bi_2Se_3	0.0%	0.2900 eV	(−)	++−− +−++ −−+− ++−− +−++ −−++ −−+− +−+− +−+− −+−+ −+;−
	+4.0%	0.1300 eV	(−)	++−− +−++ −−+− ++−− +−++ −−++ −−+− +−++ −−+− −+−+ −+;−
	+5.8%	0.0005 eV	(−)	+$\widehat{+−−+}$−+$\widehat{+−−+}$− +$\widehat{+−−+}$−+$\widehat{+−−+}$− +$\widehat{−+}$− $\widehat{−+}$+$\widehat{+−−+}$ $\widehat{−+}$−$\widehat{+−}$;−
	+6.0%	0.0122 eV	(+)	+$\widehat{−++−}$−+$\widehat{−++−}$− +$\widehat{−++−}$−+$\widehat{−++−}$− +$\widehat{+−}$− $\widehat{+−}$+$\widehat{−+}$−+$\widehat{−}$ $\widehat{+−−+}$−;+
	+8.0%	0.1300 eV	(+)	+−++ −−+− ++−− +−++ −−+− ++−− ++−− +−+− +−+− +−−− +−;+

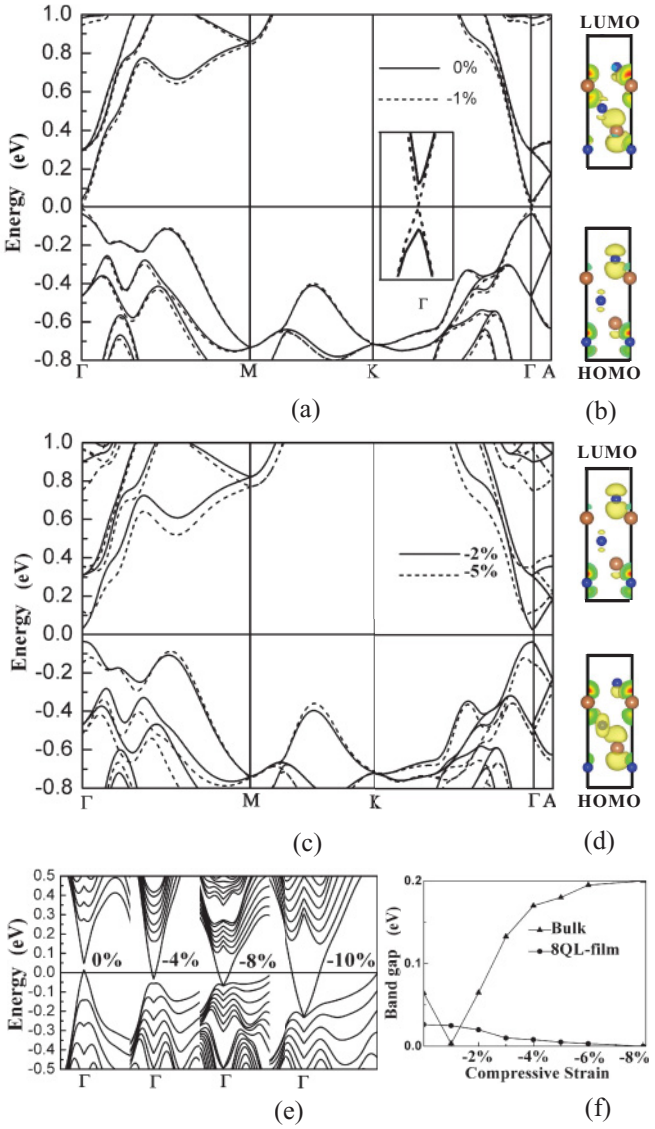

FIG. 1. (Color online) (a) and (c) Evolution of the band structure of bulk Sb_2Se_3 under compressive strain along the c axis from -1% to -5%. The corresponding parity eigenvalues under these strains are listed in Table I. The inset in (a) is a close-up view of the bands near the Γ point. (b) and (d) The charge distributions of the HOMO and LUMO at the Γ point under strains of 0% and -2%, respectively. The LUMO and HOMO charge distributions under a strain of -1% (-5%) are very similar to those under a strain of 0% (-2%). The brown (blue) spheres denote Sb (Se) atoms. (e) Band evolution of the 8-QL Sb_2Se_3 film near the Γ point with c-axis compressive strains. (f) The band gap as a function of the compressive strain applied to Sb_2Se_3 bulk and film.

interaction while it is much more dependent on the longitudinal one. Therefore, c-axis strain alone can change the topological phase while lateral strains alone cannot. However, it should be noted that a small lateral strain can induce a considerable c-axis deformation due to the small Poisson's ratio (0.25). In this way, the lateral strain can cause topological phase transition indirectly. As a confirmation, we expanded the lattice laterally by 0.5%. It is found that a -2% longitudinal strain is induced and consequently Sb_2Se_3 becomes a TI. For brevity's sake, the strain is implicitly referred to as the longitudinal c-axis strain in the following if not otherwise specified.

It is found that the c-axis strain is inhomogeneous in strained Sb_2Se_3. The QL length h_{QL} changes little while the inter-QL separation d_{QL} is reduced much more under compressive strain. For instance, when a Sb_2Se_3 bulk unit cell is compressed by 2% along the c axis, h_{QL} is shortened by only 0.3% whereas d_{QL} is compressed by 5.81%. This is because the atomic layers within a QL are strongly covalently bonded, while the inter-QL interaction is weak van der Waals interaction, resulting in inhomogeneous strain. It is interesting to examine which induces the topological phase transition: the intra- or inter-QL compression. We first keep h_{QL} unchanged and reduce d_{QL} by 5.81%. Parity analysis shows that this hypothetical system is a TI. We also studied an opposite hypothetical system where d_{QL} is fixed while h_{QL} is reduced from 0.3% to 2%. It is found that this system remains an NI. Therefore, the topological phase is primarily dependent on the inter-QL interaction.

Since compressive strain can turn Sb_2Se_3 into a TI, one can imagine tensile strain can convert Bi_2Se_3 into an NI. Our parity analysis on both bulk unit cells of Bi_2Se_3, i.e., the 5-atom primitive cell and the 3-QL 15-atom hexagonal cell, indicates that unstrained Bi_2Se_3 is a TI, in agreement with the previous studies.[11,25] The band gap is found to be 0.29 eV, close to the experimental value and other calculations. A tensile strain ranging from 1% to 10% is applied along the c axis of bulk Bi_2Se_3. The Poisson's ratio of Bi_2Se_3 is calculated to be 0.24. In Fig. 2(f), one can see that the band gap first becomes smaller and then larger with the increase of tensile strain, indicating a TI-to-NI transition. The transition point is found to be around 6%. In Table I, one can see that the sign of the product of the parities of the occupied bands changes from negative to positive between strains of 5% and 6%. We find that a strain of 5.8% is very close to the transition point. The energy gap is as small as 0.0005 eV and the system is a TI (See Table I). The previously discussed dependence of the topological phase on anisotropic interactions is confirmed in Bi_2Se_3. One may notice that the parity eigenvalues have changed significantly with a change in strain of 5.8% to 6.0%, which seems to indicate some abrupt change in the band structure for such a small variation of strain. We found that there are many nearly degenerate states at the Γ point. For example, the second and third bands are almost degenerate at the Γ point, and so are the fourth and fifth bands. When the strain is changed, the order of these nearly degenerate bands can be switched and parity will be changed accordingly. We have marked the nearly degenerate bands in Table I at strains of $+5.8\%$ and $+6\%$. It can be seen that all the changes of parity occur within the nearly degenerate bands.

B. The topological phase transition in thin films

The highlight of TIs is their Dirac cone of protected topological surface states, which can only be realized in the surface or in films. Almost all new applications of TIs are related to these special surface states. It is highly desirable to determine if they can be tuned by some means in a controllable way.

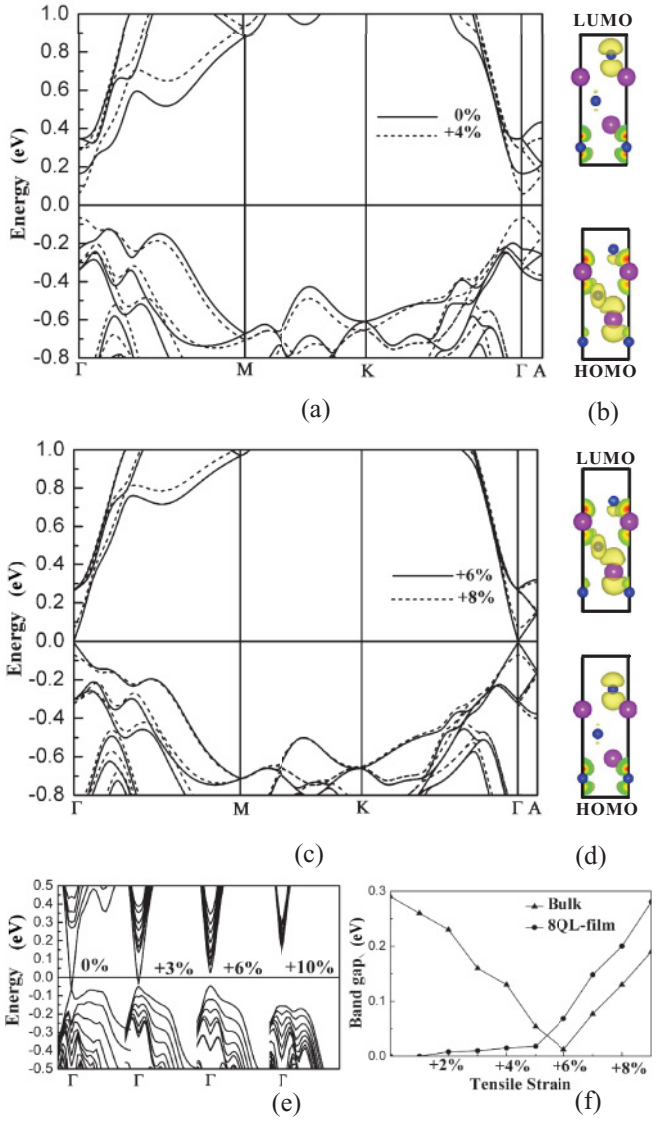

FIG. 2. (Color online) (a) and (c) Evolution of the band structure of bulk Bi_2Se_3 under tensile strain along the c axis from 0% to 8%. The corresponding parity eigenvalues under these strains are listed in Table I. (b) and (d) The charge distributions of the HOMO and LUMO at the Γ point under strains of 0% and 6%, respectively. The LUMO and HOMO charge distributions under a strain of 4%(8%) are very similar to those under a strain of 0%(6%). The purple (blue) spheres denote Bi (Se) atoms. (e) Band evolution of the 8-QL Bi_2Se_3 film near the Γ point under c-axis tensile strains. (f) The band gap as a function of the tensile strain applied to Bi_2Se_3 bulk and film.

For this purpose, we investigated how the surface bands of Sb_2Se_3 respond to strain. The surface is modeled by an 8-QL slab in our calculation. With the increase of compressive strain, the band gap becomes smaller and smaller. It vanishes when the strain reaches −8% [Fig. 1(e)], signaling the formation of topological metallic surface states. Since we have shown above that bulk Sb_2Se_3 is turned into a TI under a strain of −2%, one might expect that, in the semi-infinite surface of Sb_2Se_3 under the same strain, the topological metallic surface band should appear. However, our calculations show that the surface band gap remains open before the strain exceeds −8%. The difference of the calculated (−8%) and the expected (−2%) gap closure points can be ascribed to the difference between the thickness of the 8-QL film and the semi-infinite Sb_2Se_3 surface. The SOC is weaker in the former than in the latter, and hence larger compressive strain is required to turn the former in to a TI.

We also calculated the band structure of the 8-QL Bi_2Se_3 film under tensile strains, as shown in Fig. 2(e). As can be seen, the band gap is opened and grows larger with the increase of the tensile strain. The topological surface metallic states are turned into normal insulating surface states.

Our investigation of the TI films is related to the important issue of the interaction of the opposite surfaces of thin films. In previous experimental and theoretical studies, it was thought that the coupling of the two opposite surfaces of thin films would open up a gap in the Dirac cone of the surface bands.[27–29] If this supposition is true, the application of compressive c-axis strain to the thin films, which would reduce the distance of the two surfaces and increase the coupling between them, will lead to larger band gap. In contrast, our calculations show that the compressive strain will reduce the band gap of the surface states and can lead to an NI-to-TI phase transition. This is because the topological phase is mainly dependent on the inter-QL distance and reduction of inter-QL distance by compressive strain can increase spin-orbit coupling. The band gap is open only when c-axis tensile strain is applied to the thin film.

IV. CONCLUSION

In conclusion, we have investigated the dependence of topological phase on the anisotropic interactions in Bi_2Se_3-type materials. It is revealed that the inter-QL interaction, instead of the lateral interaction and intra-QL interaction, is a dominant mechanism for determining the topological phase. The strain can modulate the crystal field as well as SOC. We explain the topological phase difference of Sb_2Se_3 and Bi_2Se_3 and propose a practical means to tune the topological phase by strain. It is found that Sb_2Se_3 can be converted into a topological insulator by applying compressive longitudinal strain while the converse strain can turn Bi_2Se_3 into a normal insulator. The strained films are also studied and it is found that their topological surface states can also be tuned accordingly. The interaction of the opposite surfaces of TI films is clarified. Our results have important implications for experiments, where strain widely exists at surfaces and interfaces,[3,27,30–34] leading to a change of topological phase.

ACKNOWLEDGMENTS

The authors acknowledge the support of the National Natural Science Foundation of China (Grants No. 11074211, No. 10874143, and No. 10974166), the Education Foundation of Science and Technology Innovation of the Ministry of Education, China (Grant No. 708068), the Research Foundation of Education Bureau of Hunan Province, China (Grants No. 10A118, No. 09K033, and No. 09A094), and the Program for New Century Excellent Talents in University (Grant No. NCET-10-0169).

*xiangyang_peng@xtu.edu.cn
†jxzhong@xtu.edu.cn

[1] Y. Xia, D. Qian, D. Hsieh, L. Wray, A. Pal, H. Lin, A. Bansil, D. Grauer, Y. S. Hor, R. J. Cava, and M. Z. Hasan, Nat. Phys. **5**, 398 (2009).
[2] Y. L. Chen, J. G. Analytis, J. H. Chu, Z. K. Liu, S. K. Mo, X. L. Qi, H. J. Zhang, D. H. Lu, X. Dai, Z. Fang, S. C. Zhang, I. R. Fisher, Z. Hussain, and Z. X. Shen, Science **325**, 178 (2009).
[3] G. H. Zhang, H. J. Qin, J. Teng, J. D. Guo, Q. L. Guo, X. Dai, Z. Fang, and K. H. Wu, Appl. Phys. Lett. **95**, 053114 (2009).
[4] T. Zhang, P. Cheng, X. Chen, J. F. Jia, X. Ma, K. He, L. Wang, H. Zhang, X. Dai, Z. Fang, X. Xie, and Q. K. Xue, Phys. Rev. Lett. **103**, 266803 (2009).
[5] C. L. Kane and E. J. Mele, Phys. Rev. Lett. **95**, 146802 (2005).
[6] M. Z. Hasan and C. L. Kane, Rev. Mod. Phys. **82**, 3045 (2010).
[7] X. L. Qi and S. C. Zhang, Phys. Today. **63**, 33 (2010).
[8] B. A. Bernevig, T. L. Hughes, and S. C. Zhang, Science **314**, 1757 (2006).
[9] I. Garate and M. Franz, Phys. Rev. Lett. **104**, 146802 (2010).
[10] L. Fu and C. L. Kane, Phys. Rev. Lett. **100**, 096407 (2008).
[11] H. J. Zhang, C. X. Liu, X. L. Qi, Z. Fang, and S. C. Zhang, Nat. Phys. **5**, 438 (2009).
[12] S. S. Hong, W. Kundhikanjana, J. J. Cha, K. J. Lai, D. Kong, S. Meister, M. A. Kelly, Z. X. Shen, and Y. Cui, Nano Lett. **10**, 3118 (2010).
[13] J. H. Song, H. Jin, and A. J. Freeman, Phys. Rev. Lett. **105**, 096403 (2010).
[14] O. V. Yazyev, J. E. Moore, and S. G. Louie, Phys. Rev. Lett. **105**, 266806 (2010).
[15] Y. L. Chen, J. G. Analytis, J. H. Chu, Z. K. Liu, S. K. Mo, X. L. Qi, H. J. Zhang, D. H. Lu, X. Dai, Z. Fang, S. C. Zhang, I. R. Fisher, Z. Hussain, and Z. X. Shen, Science **329**, 659 (2010).
[16] D. Teweldebrhan, V. Goyal, and A. A. Balandin, Nano Lett. **10**, 1209 (2010).
[17] S. M. Young, S. Chowdhury, E. J. Walter, E. J. Mele, C. L. Kane, and A. M. Rappe, Phys. Rev. B **84**, 085106 (2011).
[18] D. Xiao, Y. G. Yao, W. X. Feng, J. Wen, W. G. Zhu, X. Q. Chen, G. M. Stocks, and Z. Y. Zhang, Phys. Rev. Lett. **105**, 096404 (2010).
[19] S. Chadov, X. L. Qi, J. Kübler, G. Fecher, C. Felser, and S. C. Zhang, Nat. Mater. **9**, 541 (2010).
[20] G. Kresse and J. Furthmüller, Phys. Rev. B **54**, 11169 (1996).
[21] G. Kresse and J. Furthmüller, Comput. Mater. Sci. **6**, 15 (1996).
[22] J. P. Perdew, K. Burke, and M. Ernzerhof, Phys. Rev. Lett. **77**, 3865 (1996).
[23] P. E. Blöchl, Phys. Rev. B **50**, 17953 (1994).
[24] L. Fu and C. L. Kane, Phys. Rev. B **76**, 045302 (2007).
[25] W. Zhang, R. Yu, H. J. Zhang, X. Dai, and Z. Fang, New. J. Phys. **12**, 065013 (2010).
[26] W. Cheng and S. F. Ren, Phys. Rev. B **83**, 094301 (2011).
[27] Y. Zhang, K. He, C. Z. Chang, C. L. Song, L. L. Wang, X. Chen, J. F. Jia, Z. Fang, X. Dai, S. W. Y., S. Q. Shen, Q. Niu, S. C. Zhang, X. C. Ma, and Q. K. Xue, Nat. Phys. **6**, 584 (2010).
[28] H. Z. Lu, W. Y. Shan, W. Yao, Q. Niu, and S. Q. Shen, Phys. Rev. B **81**, 115407 (2010).
[29] C. X. Liu, H. J. Zhang, B. H. Yan, X. L. Qi, T. Frauenheim, X. Dai, Z. Fang, and S. C. Zhang, Phys. Rev. B **81**, 041307(R) (2010).
[30] Y. Y. Li, G. Wang, X. G. Zhu, M. H. Liu, C. Ye, X. Chen, Y. Y. Wang, K. He, L. L. Wang, X. C. Ma, H. J. Zhang, X. Dai, Z. Fang, X. C. Xie, Y. Liu, X. L. Qi, J. F. Jia, S. C. Zhang, and Q. K. Xue, Adv. Mater. **22**, 4002 (2010).
[31] C. L. Song, Y. L. Wang, Y. P. Jiang, Y. Zhang, C. Z. Chang, L. L. Wang, K. He, X. Chen, J. F. Jia, Y. Y. Wang, Z. Fang, X. Dai, X. C. Xie, X. L. Qi, S. C. Zhang, Q. K. Xue, and X. C. Ma, Appl. Phys. Lett. **97**, 143118 (2010).
[32] J. Chen, H. J. Qin, F. Yang, J. Liu, T. Guan, F. M. Qu, G. H. Zhang, J. R. Shi, X. C. Xie, C. L. Yang, K. H. Wu, Y. Q. Li, and L. Lu, Phys. Rev. Lett. **105**, 176602 (2010).
[33] A. Richardella, D. M. Zhang, J. S. Lee, A. Koser, D. W. Rench, A. L. Yeats, B. B. Buckley, D. D. Awschlom, and N. Samarth, Appl. Phys. Lett. **97**, 262104 (2010).
[34] C. Zhang, L. Sun, Z. Chen, X. Zhou, Q. Wu, W. Yi, J. Guo, X. Dong, and Z. Zhao, Phys. Rev. B **83**, 140504(R) (2011).